applied sciences

MDPI

Article

Pulsed Propulsion of Unmanned Aerial Vehicles by Centrifugal Force Modulation—First-Order Theory and Practicability

Wolfgang Holzapfel

Faculty of Mechanical Engineering, University of Kassel, 34109 Kassel, Germany; wolfgang.holzapfel@uni-kassel.de

Abstract: A novel technique suitable for the propulsion of small unmanned aerial vehicles (UAV) is discussed in this paper. This approach utilizes the rotational energy of airborne gyro rotors and converts it into translational propulsion for the vehicle. The energy conversion is achieved by generating precisely directed centrifugal force pulses through short-duration rotor unbalances. The accurate control of the timing and magnitude of these unbalances is crucial for successful propulsion generation. Our first-order theory of controlled unbalance propulsion (CUP) predicts the potential for achieving high translational accelerations and vehicle velocities up to orbital levels. Power-saving levitation of UAVs can be attained. In this paper, we provide traceable evidence that pulsed centrifugal propulsion is based on well-established laws of physics and can be realized using state-of-the-art technologies.

Keywords: unmanned aerial vehicles; vehicle propulsion; controlled unbalance propulsion; energy storage/conversion; high-speed rotors; centrifugal force modulation

Citation: Holzapfel, W. Pulsed Propulsion of Unmanned Aerial Vehicles by Centrifugal Force Modulation—First-Order Theory and Practicability. *Appl. Sci.* **2024**, *14*, 4229. https://doi.org/10.3390/app14104229

Academic Editor: Jérôme Morio

Received: 1 March 2024
Revised: 22 April 2024
Accepted: 25 April 2024
Published: 16 May 2024

1. Introduction

The idea of generating propulsion through rotating unbalance is by no means new. In the patent literature, there are already various approaches for so-called centrifugal force drives that propose the use of rotors with asymmetric mass distribution, e.g., [1–4]. However, these have so far not led to any functional realizations. The proposed methods are controversial in the scientific community, not least because they seem to violate the physical law of conservation of momentum and because the rotating centrifugal force, as a pseudo force, could not cause a lasting translation of the rotor's center of mass. Currently, there are apparently no contributions or discussions on this topic in reputable scientific journals. There is nothing told about this inertial technology in actual publications [5–7], which review the state of the art in different propulsion technologies for unmanned aerial vehicles (UAV). On the other hand, it is well known that the rotational energy of masses can be successfully utilized for energy storage purposes, as seen in [8–12], as well as the online contribution [13] by the Max Planck Institute for Plasma Physics. An up-to-date overview of the design and optimization of flywheel energy storage systems in automotive engineering is available in reference [14].

This paper presents to our knowledge the first attempt at quantitative designing a centrifugal force drive that utilizes (1st) flywheel energy storage and (2nd) transfers that energy by controlled flywheel unbalance modulation into vehicle movement. Thus, the flywheel on board the vehicle serves as well for energy storage as for vehicle propulsion, too. It is based on known laws of physics, and therefore, such a drive will work in principle. It is shown that a basic requirement for a functional drive is the precise spatial rectification of the vector of the resulting centrifugal force. This, in turn, can be achieved by a rapid temporal impulse modulation of the unbalance-induced force amplitude. To understand such functional drives and discuss the fundamental problems of flywheel propulsion, we have to remember here the relevant physical facts and laws [15–17]:

The law of conservation of angular momentum states that the total angular momentum in a closed rotation system remains constant. Therefore, if no external forces act on the system, the total angular momentum remains unchanged. However, if a force causes an acceleration of the system's mass, the angular velocity and hence the angular momentum will change.

In contrast, there is no general conservation law for rotational energy. This is because rotational energy depends on the type of forces and torques acting on the system. If there are no external forces or torques act on the system, the rotational energy remains constant. However, if forces or torques are present and cause linear acceleration of the system, rotational energy is converted into translational energy. If rotational energy is converted into other forms of energy while the angular momentum of the system remains constant, then either the moment of inertia or the rotational axis of the system must change. However, if the rotational axis remains unchanged and the moment of inertia remains constant, then the conversion of rotational energy into other forms of energy will result in a change in the angular momentum of the system. This is caused by the fact that rotational energy changes due to a change in angular velocity.

Only physical forces acting on an object from outside are considered real forces in classical physics. These external forces are caused by a direct interaction between the bodies involved and are described, for example, by the law of gravity or Coulomb's law. However, additional forces are observed as a result of translational or rotational acceleration of the reference system: inertial force, centrifugal force, Coriolis force, and Euler force. Only the acceleration-free reference systems remain free of these additional forces by definition, which are called inertial reference systems. At first, the physics of the 19th century taught that these forces were not natural (real) forces but so-called pseudo forces that appeared in mathematical coordinate transformations. Referring to centrifugal forces, which are particularly important in this work, it was said that centrifugal forces are internal reactions that occur during rotation. The total momentum of the system cannot be changed by the internal forces of the system. Thus, if no external forces act on the system and also system energy remains constant, then, according to the law of conservation of momentum, the total momentum of the system remains constant. This would mean here that inertial propulsion forces could not occur. An inertial propulsion device would not be technically useful.

However, current physics tends to consider this strict distinction between internal and external forces as incorrect and recognizes that, for example, centrifugal forces are not only apparent but can also cause devastating destruction in rotating systems [17]. Examples from practical mechanical engineering are rotor cracks that occur at high rotation speeds and from experimental atomic physics: atomic collisions with angular momentum transfer, where the strong force of the atomic nuclei is overcome by centrifugal forces. Currently, theoretical physics cannot assign these dynamic effects of pseudo forces to the four fundamental force interactions, nor can they be derived from the general theory of relativity.

Therefore, in compliance with current physics and for engineering considerations, we will treat centrifugal forces like real physical forces in this paper. This is not only due to the fact that the centrifugal "pseudoforce" can break steel rotors, but we also have evidence that this force can accelerate rotor masses and propel vehicles if its magnitude and spatial direction are strictly controlled. To achieve such real vehicle propulsion, the rotating centrifugal force must be converted into directed centrifugal force. This conversion is achieved through pulse amplitude modulation, which must be performed strictly synchronously with rotor rotation. By doing this, directed centrifugal force will produce a directed acceleration of the rotor. Thus, the rotational energy of the disc is converted into translational energy, leading to the directed translational acceleration of the vehicle by utilizing the starting energy or starting angular momentum of the disc. We will clarify this through mathematics in the following chapters of the paper. The final falsification of this assumption must be reserved for later experiments.

The paper is structured as follows: In Section 2, we present a first-order theory as the basis for our subsequent analysis. In Section 3, we derive energy conversion formulas, which will allow us in Section 4 to make rough estimates of the flight performance of propulsion systems. Next, in Section 5, we discuss the ability of inertial-driven UAVs in terms of maneuverability and levitation. Sections 6 and 7 cover the need for precise control in activating and deactivating rotor unbalances, as well as the use of high-strength rotor materials. Finally, our conclusions on the pulsed propulsion of UAVs are presented in Section 8.

2. First Order Theory of Propulsion Generation by Means of Rotation Energy

Assume a stiff rotor disc (radius R, thickness D < R, homogenic material distribution, total mass M) equipped with fixed unbalanced mass m_u at its periphery (Figure 1). The disc rotation axis A should be perpendicularly centered in a planar system with orthogonal axes (x; y), fixed in an inertial reference frame. We apply in the following discussion the equivalent circuit mass point diagram of Figure 1 (right).

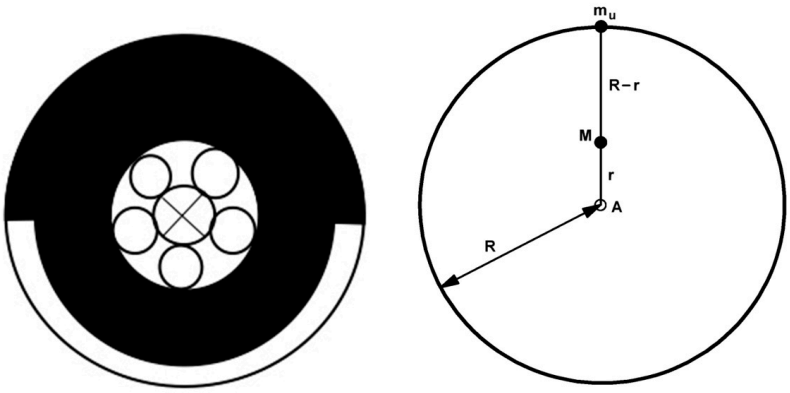

Figure 1. (**Left**): Unbalanced rotor due to asymmetric mass distribution. (**Right**): equivalent circuit mass point diagram [18] with A rotation axis, perpendicular to paper plane (x; y), m_u point of unbalance mass, M point of rotor disc mass, R rotor radius, r translation of M due to m_u.

Due to disc rotation, the generated centrifugal force vector written in polar coordinates is

$$\begin{aligned} \vec{F}_u &= \vec{R} m_u \omega^2 \\ \vec{R} &= R e^{i(\omega t + \varphi_0)} \end{aligned} \tag{1}$$

with magnitudes

$\vec{R}$ radius vector (i = imaginary unit) pointing from axis A to unbalance mass m_u
φ_0 rotor fixed azimuth of the unbalanced mass point m_u
R radius of the rotor disc
$\omega = 2\pi f$ (angular) revolution frequency
$T = \frac{1}{f}$ cycle time of rotor disc

Equation (1) says centrifugal force vector $\vec{F}_u$ is always pointing in the direction of instantaneous $\vec{R}$. Its magnitude F_u increases proportional with m_u and proportional with rotor radius R, furthermore, F_u is increasing quadratically with applied rotor rotation frequency f.

It is useful to introduce an unbalance vector $\vec{U}$ that is vector $\vec{F}_u$ divided by the square of angular rotation frequency ω:

$$\vec{U} = U_0 e^{i(\omega t + \varphi_0)} = m_u R e^{i(\omega t + \varphi_0)} \tag{2}$$

Note, unbalance magnitude $U_0 = m_u R$ is independent of ω. Due to peripheric unbalance mass m_u there is a small displacement r of disc gravity center M arises, away from rotor rotation axis A. Note that this displacement is caused due to static balancing of the rigged disc. Additionally, the elasticity and strain of real rotor materials may contribute to real displacement, but we will not take this effect into account here.

In the case of very small unbalance mass m_u (i.e., $M = M_0 + m_u$, $m_u \ll M_0 \cong M$), the following vector equation results:

$$M\vec{r} = m_u\vec{R} \tag{3}$$

respectively, for the magnitudes

$$Mr = m_u R$$

According to Equation (3) the displacement r points always towards peripheric unbalance mass m_u. Thus, rotation axis A, disc mass M, and unbalanced mass point m_u are located on the same radius vector R (azimuth φ_0). Considering this we draw the conclusion: Vectorial displacement r of gravity center M can be controlled in principle via choosing magnitude and azimuth of the peripheric unbalance mass m_u!

Now the question arises: Is this mass displacement effect insignificantly small or can it be used to the best advantage in propulsion technology?

To give the answer in Figure 2, the centrifugal force F_u is represented in two orthogonal components:

$$F_{ux} = F_u \cos\varphi_x \text{ (effective centrifugal force component, see below)} \tag{4}$$

$$F_{uy} = F_u \sin\varphi_x \text{ (noneffective centrifugal force component, see below)} \tag{5}$$

$$\varphi_x = \omega t \pm mod\ 2\pi \text{ instantaneous phase angle, } t = 0 : \varphi_x = 0$$
$$t = T : \varphi_x = 2\pi$$

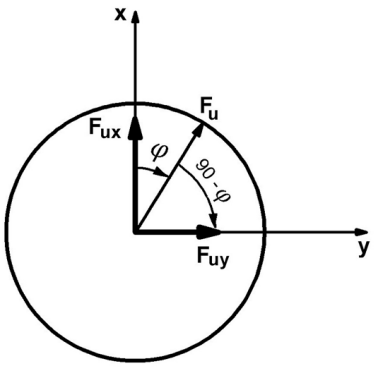

Figure 2. Components of centrifugal force vector. F_u instantaneous centrifugal vector. F_{ux} effective x-component of F_u. F_{uy} noneffective-component of F_u. φ instantaneous rotation angle of F_u against x.

Both components describe strictly harmonic forces having zero averages over each rotation period, i.e.,

$$F_x = \frac{1}{2\pi}\int_0^{2\pi} F_{ux} d\varphi = 0$$
$$F_y = \frac{1}{2\pi}\int_0^{2\pi} F_{uy} d\varphi = 0$$

Our approach to solve the problem how to obtain a non-zero resulting translatoric propulsion of the rotating disc: (partial) rectification of centrifugal force must be realized. To explain the need for force rectification, let us assume here that wanted propulsion should appear in the x-direction. Consequently, we have to modulate unbalance during each rotation in the following way (Figure 3):

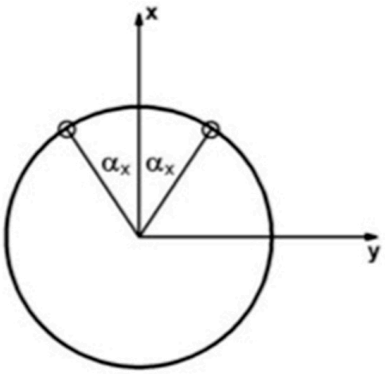

Figure 3. Active angle interval $2\alpha_x$ symmetric to thrust direction x.

In an azimuthal angle region $2\alpha_x$ highly symmetric to the x-axis, i.e., the wanted propulsion direction, we generate non-zero unbalance. Otherwise, outside of this region, i.e., in the remaining region $2\pi - 2\alpha_x$, this unbalance is always compensated. Thus, we have to switch on and off the rotor unbalance within time period τ, which is only a small fraction of cycle time T

$$\frac{\tau}{T} = \frac{2\alpha_x}{2\pi}$$

To achieve this, unbalances are selectively generated, for example, by rotor-fixed actuators, so that the resulting pulsating centrifugal forces cause a directed propulsion of the rotor mass and, thus, the flying object via the rotor bearings. If we succeed in managing this ultrafast modulation due to rotation, we obtain a train of force impulses, each pulse of duration τ and separated by cycle time T from each other. This impulse train will result in a significant change of the translational state of rotor mass M: According to Newton, force F acting on mass point M equals the first derivate of its translational impulse $P = M_v$ (v = translational velocity), thus

$$\begin{array}{c} \frac{dP}{dt} = F(t) \\ \Delta P = M\Delta v = F(t)\Delta t \end{array} \tag{6}$$

The resulting impulse change during each rotation follows from

$$\Delta P = \int_{-\frac{\tau}{2}}^{\frac{\tau}{2}} F(t)dt = 2\int_{0}^{\frac{\tau}{2}} F(t)dt$$

We obtain the effective impulse component (x-component} of centrifugal force:

$$F(t) = F_{ux}(t) = F_u \cos \omega t$$

$$\Delta P_x = \int_{0}^{T} F_u \cos \omega t dt = \int_{-\frac{\tau}{2}}^{\frac{\tau}{2}} F_u \cos \omega t dt$$

$$\Delta P_x = 2\int_{0}^{\frac{\tau}{2}} F_u \cos \omega t dt = 2\left(\frac{F_u}{\omega}\right)\sin\frac{\omega\tau}{2} \tag{7}$$

Otherwise, due to the (ineffective) y-component of centrifugal force, zero average of impulse change is confirmed:

$$F_{uy} = F_u \sin \varphi_x$$

$$\Delta P_y = \int_{-\frac{\tau}{2}}^{\frac{\tau}{2}} F_{uy} d\varphi = 0 \tag{8}$$

Let us assume the angle of unbalance activity (Figure 3)

$$\alpha_x \leq \frac{\pi}{2}, \ \sin\alpha_x \leq 1$$

we can rewrite (7) to obtain the non-zero force magnitude in the x-direction

$$F_x = 4\pi m_u R f^2 \sin\alpha_x = m_u R \omega^2 \frac{\sin\alpha_x}{\pi} \tag{9}$$

Based on Equations (7)–(9) above we conclude in summary:

The magnitude of propulsion force depends linearly on rotor radius R and on unbalance mass m_u and increases with the square of rotational frequency f. For fixed values of unbalance mass m_u, rotor radius R and rotation frequency f propulsion force F_x will become its maximum if the unbalance is present in an angle range of $2\alpha_x = 180^\circ$. Furthermore, due to our intermitted operation of rotor unbalance, only the wanted outward force component F_x (propulsion force) occurs in the rotation plane. The propulsion force, F_x, is orthogonal to rotation axis A and points exactly in the wanted direction, x, which is in a symmetrical position within an unbalance activity angle $2\alpha_x$. On the other hand, the orthogonal force component F_y is extinguished over each rotation period. If there is no other restriction, the unchained rotor will move exactly in direction x of the only acting force F_x. Its start point is $x = 0$ at time $t = 0$.

Here follows our description of the takeoff scenario:

The UAV containing the well-balanced rotor on board is initially fixed in a constraining device at the start position. After electrical loading, the rotor spins with a high rotation frequency. The translational energy of the fixed rotor is zero at the beginning of the start phase because all kinetic energy is stored in rotation energy. If we now generate a permanent unbalance mass on the spinning rotor, it will produce only rotating centrifugal force and unwanted vibrations of the cell and constraining device. But by controlled on/off-unbalance activation always in the same selected angle range during each revolution, a sequence of force pulses in the wanted direction is generated due to permanent rotation which can be used now to produce directed propulsion of the vehicle cell. Thus, after opening the constraining device, the directed force pulse sequence will produce the translational acceleration and cause movement of the UAV away from its start position.

For simplicity in the dynamic situation, we are assuming here the subcritical operation of the rotor system itself: the lowest resonance frequencies are all above the rotational frequency f of the rotor. All critical system components (actuators, rotor bearings, etc.) are assumed to be sufficiently hard; thus, superimposed elastic forces and friction forces in the system are eliminated. During free flight, only inertial forces act on the rotor bearing, as the elastic mounting forces are eliminated when the rotor is detached. As a result, the load on the bearings due to unbalance is significantly lower during flight than when operating a tethered rotor, which has a favorable effect on the bearing life.

3. Conversion of Rotational Energy into Translational Vehicle Energy

Pulsed propulsion by centrifugal force modulation can be applied in two modes of rotor energy management:

(1) The rotor could be used with an integrated onboard drive, able to deliver high and sustained electrical power output during the complete mission. Low weight and compact design of such a combined power/propulsion system well suited onboard a small UAV must be achieved here, which is not even an easy engineering task;
(2) Alternatively, the rotor will be brought to operating speed before takeoff through temporary mechanical coupling with a powerful external electric motor. The advantage of

this pure inertial solution is its much lower weight and more simplicity of the onboard propulsion system. But here the question arises: is there enough energy onboard such a UAV, and how much is its flight performance and maneuverability limited?

We will focus here on the management of this second energy mode because it seems better suited for small UAVs, at least in the present state of technology. Furthermore, if the successful combination of (1) and (2) would be feasible in the future, our focus will deliver advanced performance.

When discussing the conversion of rotational energy (E_{rot}) into translational energy (E_{trans}) in the context of a UAV, it is important to consider the conservation of total kinetic energy (E_0) onboard the vehicle. According to the energy theorem, the total kinetic energy must remain constant. Therefore, we can express this conservation using the following Equation:

$$E_0 = E_{rot} + E_{trans} = const. \tag{10}$$

At the beginning of the takeoff scenario, when the UAV is at the starting point ($x = 0$), the maximum rotational energy is available. This can be represented as follows:

$$\max E_{rot} = \frac{1}{2}\theta\omega_0^2 = E_0 \tag{11}$$

with the moment of disc inertia

$$\theta = \frac{1}{2}MR^2$$

and a maximum of rotation frequency:

$$\omega_0 = 2\pi f_0$$

According to (11), storable rotation energy increases proportional to rotor mass M and with the square of the disk radius R and square of rotation frequency f_0. Thus, for a given size and material of the rotor disk, a doubling of its rotation frequency f_0 will result in a quadruple of mechanically stored airborne energy. Our conclusion: The store parameter f_0 is of high importance in flight performance evaluation. As per Equation (11), the amount of storable rotational energy increases proportionally with the rotor mass (M), the square of the disk radius (R^2), and the square of the rotation frequency f_0. Therefore, if the rotation frequency f_0 is doubled while keeping the size and material of the rotor disk constant, the mechanically stored airborne energy will quadruple. This highlights the significance of the rotation frequency (f_0) as a parameter in evaluating flight performance (refer to Section 4 for more details).

On the other hand, assuming ideal conditions in energy conversion, i.e., friction-free disc rotation and vehicle translation) and zero gravity space, the potential maximum of translational energy appearing at the end of energy conversion is given by

$$\max E_{tran_s} = E_0 = \frac{1}{2}M' v_{max}^2 = MR^2\pi^2 f_0^2 \tag{12}$$

This assumption is equivalent to 100% efficiency in the conversion of the rotational energy to translational propulsion. It is also important to note that M' is larger than M, as M' represents the total mass of the UAV while M only represents the smaller mass of the rotor disc. The vehicle construction factor C, which is the ratio of M' to M, can be assumed to be between 1 and 2 in realistic scenarios.

Thus, the maximum translational velocity is as follows:

$$v_{max} = \frac{1}{\sqrt{2}}R\omega_0\sqrt{\frac{M}{M'}} \tag{13}$$

Maximum velocity v_{max} depends on radius R, angular velocity ω_0, and construction factor $C = \frac{M'}{M}$; however, v_{max} is independent of the unbalance mass m_u.

We are looking now at intermediate states of energy transformation: Energy theorem postulates that each increase in translational energy asks for an equal decrease in rotational energy, i.e.,

$$-dE_{rot} = dE_{trans} \tag{14}$$

$$E_{rot} = \frac{1}{4}MR^2\omega^2 \tag{15}$$

$$E_{rot} = \frac{1}{4}MR^2 2\omega d\omega = \frac{1}{2}MR^2\omega d\omega \tag{16}$$

$$E_{trans} = \frac{1}{2}M'v^2 \tag{17}$$

$$-\frac{1}{2}MR^2\left(\frac{d\omega}{dt}\right) = M'v\left(\frac{dv}{dt}\right) \tag{18}$$

$$-\frac{1}{2C}R^2\omega\left(\frac{d\omega}{dt}\right) = va \tag{19}$$

Equation (19) teams our rotational magnitudes with the translational ones of interest, i.e., vehicle velocity v and its translational acceleration a.

The third axiom of Newton (action = reaction) tells us about acceleration a of mass: Centrifugal force $F = m_u R\omega^2$ caused by unbalance and inertial force $F = M'a = M'\frac{d^2x}{dt^2}$ acting on vehicle mass M' must be in equilibrium, i.e.,

$$M'a = m_u R\omega^2 \tag{20}$$

Thus, we obtain the acceleration $\left(a = \frac{dx^2}{dt^2} = \frac{dv}{dt}\right)$ of vehicle mass M':

$$a = \left(\frac{m_u}{M'}\right)R\omega^2 \tag{21}$$

From (19) follows the time-dependent change of rotation frequency:

$$\frac{d\omega}{dt} = -\frac{2Cva}{R^2}\omega = -2\left(\frac{m_u}{MR}\right)v\,\omega$$

$$\frac{d\omega}{\omega} = -2\left(\frac{m_u}{MR}\right)vdt \tag{22}$$

After integration, we have the following:

$$ln\omega - ln\omega_0 = -2\left(\frac{m_u}{MR}\right)\int_0^x vdt \tag{23}$$

$$\frac{ln\,\omega}{\omega_0} = ln\frac{f}{f_0} = -2\left(\frac{m_u}{MR}\right)x \tag{24}$$

We obtain instantaneous rotation frequency in dependence of $x = x(t)$, which is the trajectory length depending on trust duration time t:

$$\omega = \omega_0\, exp\left\{\left(-\frac{2m_u}{MR}\right)x\right\},\ resp.\ \omega^2 = \omega_0^2\, exp\left\{\left(-\frac{4m_u}{MR}\right)x\right\}. \tag{25}$$

Rotation frequency decreases exponentially with increasing $x(t)$. This follows from the increase in translational energy and instantaneous velocity v (see Figure 4):

$$E_{trans} = E_0 - E_{rot}$$

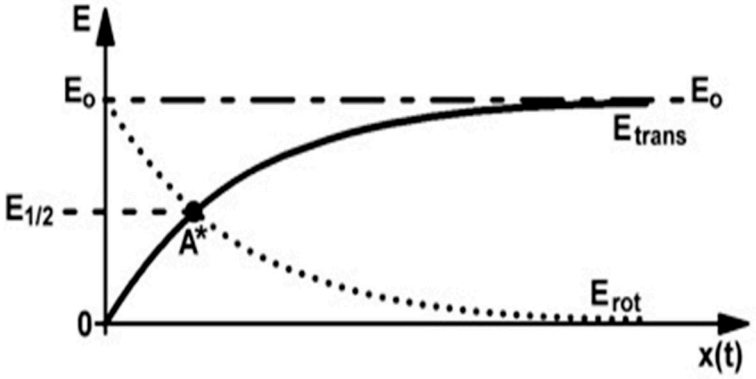

Figure 4. Decrease in rotational energy E_{rot} and increase in translational energy E_{trans} in dependence of flight path length $x(t)$. E_0, $E_{1/2}$: max and half-max of rotation energy, A^* Point of energetic equivalence.

With (11) and (25), we obtain via $E_0 = max\ E_{rot} = \frac{1}{4}MR^2\omega_0^2$

$$E_{trans} = \frac{1}{2}M'v^2 = \frac{1}{4}M'R^2\omega_0^2\left(1 - exp\left\{\left(-\frac{4m_u}{MR}\right)x\right\}\right) \tag{26}$$

$$v^2 = \frac{1}{2}R^2\,\omega_0^2\left(1 - exp\left\{\left(-\frac{4m_u}{MR}\right)x\right\}\right) \tag{27}$$

$$v = \frac{1}{2}\,R\,\omega_0\,\sqrt{1 - exp\left\{\left(-\frac{4m_u}{MR}\right)x\right\}} \tag{28}$$

$v(x)$ is the instantaneous velocity in dependence of trajectory length x. Setting $x = 0$ delivers initial velocity $v = 0$ in accordance with our takeoff scenario above. From (28), we obtain by differentiation the instantaneous translational acceleration of the rotor:

$$a = \left(\frac{m_u}{M'}\right)\,R\,\omega^2 = \left(\frac{m_u}{M'}\right)R\,\omega_0^2 exp\left\{\left(-\frac{4m_u}{MR}\right)x\right\} \tag{29}$$

Initial acceleration a_0 follows from (29) by setting starting point condition $x = 0$:

$$a_0 = \left(\frac{m_u}{M'}\right)R\,\omega_0^2 \tag{30}$$

Both instantaneous acceleration a and velocity x depend on mass quotient $\frac{m_u}{M'}$, which presents the main steering magnitude for propulsion control. Acceleration increases proportionally with $\frac{m_u}{M'}$.

Regarding the momentum and angular momentum laws during the energy conversion, the rotational momentum constantly decreases due to the reduction of the rotational frequency, while the translational momentum increases in magnitude due to the energy conversion accompanying the increase in translational velocity. However, it would be inappropriate to speak of a conversion of momentum, as these quantities cannot be reconciled due to the different physical dimensions of angular and translational momentum. There is a certain analogy to the behavior of a non-conservative system (e.g., a system with friction). Here, the law of conservation of energy applies, but not the law of conservation of momentum.

4. Evaluation of UAV Flight Performance Data

Our theory above applies to the five parameters M, R, f, m_u, and $C = \frac{M'}{M}$. The radius R and masses M and M' are assumed to be fixed parameters during flight, which cannot be changed. The flight performance can be controlled by precisely adjusting the active unbalance mass m_u (or $\frac{m_u}{M}$) and/or by adjusting the initial rotation rate f_0 at the start (or

the actual rotation rate f during flight). In most cases, a high initial rotation frequency f_0 is desired to store a large amount of energy on board, making the key steering parameter $\frac{m_u}{M}$.

The following formulas, derived above, are applied here for flight performance calculations:

$$\text{\# Energy mechanically stored } \; E_{rot} = MR^2 \, \frac{\omega_0^2}{4} \tag{31}$$

This formula calculates the amount of pure mechanical energy stored in the system. Energy storable on board depends on the square of radius R and square of rotation frequency f_0 and is proportional to mass M of the rotor. Any electrical power supply on board is ignored here.

There is no influence of construction factor C on the magnitude of storable rotation energy.

$$\text{\# Initial trust } \; F_0' = M' a_0' \tag{32}$$

This formula calculates the initial thrust generated by the product of the mass of the vehicle (M') and its initial acceleration (a_0')

$$\text{\# Initial acceleration } \; a_0' = \left(\frac{m_u}{M'}\right) R \, \omega_0^2 \tag{33}$$

determined by the magnitude of m_u and/or rotation frequency f_0. Typical values of $m_u = M' * 10^{-4}$, respectively $M' * 10^{-6}$, are assumed in calculation here, while f_0 is variable and R is fixed by design.

$$\text{\# Height of vertex } \; h_{max} = R^2 \frac{\omega_0^2}{g_E}. \tag{34}$$

Horizontal spin orientation of the rotor disk has to be assumed here. The height of the vertex is independent of rotor mass M and m_u. Acceleration due to Earth gravity: $g_E = 9.81 \, \frac{m}{s^2}$.

$$\text{\# Max. velocity } \; v_{max} = R \, \frac{\omega_0}{\sqrt{2}} \tag{35}$$

Vertical spin orientation of the rotor disk is assumed here. Maximum velocity is independent of rotor mass M and m_u.

For preliminary evaluation of potential in-flight performance, we take here three hypothetical UAVs of different sizes and mass and calculate the height of vertex, initial thrust, initial acceleration, and maximum velocity in dependence on initial rotation rate (Tables 1–4).

Table 1. Mini-rotor ($R = 0.125$ m, $M = 2$ kg, $m_u = M * 10^{-4}$).

Initial Frequency f_0	Hight of Vertex h_{max}	Initial Thrust F_0	Initial Acceleration a_0	Maximum Velocity v_{max}
100/s	0.640 km	10 N	5 m/s^2	56 m/s
200/s	2.560 km	40 N	20 m/s^2	110 m/s
400/s	10.200 km	160 N	80 m/s^2	220 m/s
800/s	40.800 km	640 N	320 m/s^2	440 m/s
1000/s	63.770 km	1000 N	500 m/s^2	555 m/s

All data calculated here are obtained under the simplifying assumption $M = M'$, thus $C = 1$. For the evaluation of a specific vehicle, we have to set its specific $C > 1$. Thus, initial acceleration a' and initial trust F_0' of the complete vehicle will be reduced because of bigger vehicle mass M' compared to rotor mass M. This is according to Equation $a \, M = a' M' = m_u R \omega^2$. For instance, assuming $C = 2$, the height of the vertex as well as the initial thrust of the vehicle, are smaller, namely half the value of the corresponding rotor data. Additionally, the way back to the Earth's surface and managing a safe landing needs

energy, too. However, we see no serious limitation to the flight performance. Even the minirotor should reach considerable peak heights of several kilometers or more, depending on the starting rotational frequency f_0.

Table 2. Medium-sized rotor ($R = 0.5$ m, $M = 10$ kg$\left(\textit{material density } \rho = 10\frac{\text{g}}{\text{cm}^3}\right)$, $m_u = M * 10^{-4}$).

Initial Frequency f_0	Hight of Vertex h_{max}	Initial Thrust F_0	Initial Acceleration a_0	Maximum Velocity v_{max}
100/s	10 km	200 N	20 m/s^2	220 m/s
200/s	40 km	800 N	80 m/s^2	440 m/s
400/s	160 km	3200 N	320 m/s^2	880 m/s
800/s	640 km	12,800 N	1280 m/s^2	1760 m/s
1000/s	1000 km	20,000 N	2000 m/s^2	2220 m/s

Table 3. Heavy-v sized rotor ($R = 2$ m, $M = 160$ kg, $m_u = 16$ g).

Initial Frequency f_0	Hight of Vertex h_{max}	Initial Thrust F_0	Initial Acceleration a_0	Maximum Velocity v_{max}
100/s	160 km	12,800 N	80 m/s^2	850 m/s
200/s	640 km	51,200 N	320 m/s^2	1700 m/s
400/s	2560 km	205,000 N	1280 m/s^2	3400 m/s
800/s	10,240 km	820,000 N	5120 m/s^2	6800 m/s
1000/s	16,000 km	1,280,000 N	8000 m/s^2	8500 m/s

Table 4. Heavy-sized rotor (same parameter set as above but suited for human-sized flight mode: $\frac{m_u}{M} = 10^{-6}$).

Initial Frequency f_0	Hight of Vertex h_{max}	Initial Thrust F_0	Initial Acceleration a_0	Maximum Velocity v_{max}
100/s	40 km	128 N	0.8 m/s^2	850 m/s
200/s	160 km	512 N	3.2 m/s^2	1700 m/s
400/s	640 km	2050 N	12.8 m/s^2	3400 m/s
800/s	2560 km	8200 N	51.2 m/s^2	6800 m/s
1000/s	4000 km	12,800 N	80.0 m/s^2	8500 m/s

The medium-sized rotor should already reach flight altitudes of commercial aircraft at rotational speeds of 100 per second. With the heavy-sized rotor, heights and speeds should be achievable that promise orbital capabilities.

The increase in acceleration and inertial thrust is proportional to growing ω^2. In most cases, the UAV user will not need really such high accelerations. Thus, the steering parameter $\frac{m_u}{M}$ can be reduced during the start phase (for instance, to 10^{-6}; see above the heavy-sized rotor in human-sized flight mode), and herewith, rotational energy onboard can be saved for later maneuvers.

The performance increase of the bigger rotors is easily explained as follows: The maximum height h_{max} of the rotor depends on the product of the squared radius R and the squared rotation frequency f_0, but h_{max} is independent of rotor mass M and steering parameter m_u/M. Therefore, our theory says, for instance, that the vertex height of the heavy rotor will be about 256 times larger than the vertex height of the mini rotor, assuming the same parameter values ($\frac{m_u}{M}$ and f_0) for both rotors. Note, translational velocity depends also on the product Rf_0, but linearly. Here, maximum velocity increases from 570 m/s (mini rotor) over 2.2 km/s (medium rotor) to 8.5 km/s (heavy rotor), all values calculated for top frequency 1000/s.

We conclude here that controlled unbalance propulsion (CUP) of UAVs could provide excellent flight performance data. Our calculations let us hope that high thrusts and vehicle

velocities up to orbital levels could be achieved. Thus, the working range of CUP drones could be extended to near-Earth space and is not limited to Earth's atmosphere.

5. Maneuverability of the Rotor and Levitation in a Gravitational Field

Here, a distinction is made between two states: horizontal flight and vertical flight. The orientation of the rotor's axis of rotation at takeoff determines the flight state. Due to the principle of propulsion, the axis of rotation must always be perpendicular to the future plane of movement in which the translational displacement of the rotor will occur. Within this plane of movement, the flight direction is determined by the position of the rotor sector in which the unbalance is activated, specifically by the bisector of this rotor sector. This position can be adjusted through the electrical control of the unbalance and can, therefore, be easily changed. The new position of the bisector can be set within a single rotation of the rotor, if necessary, potentially in milliseconds. This allows for rapid changes in the direction of the UAV within the x, y plane of movement (e.g., horizontal curved flight with a constant vertical axis direction). By reversing thrust, the aircraft can also decelerate (potentially with a subsequent change in flight direction) by electrically rotating the active rotor sector by 180 degrees relative to the previous direction of propulsion. In principle, no aerodynamic actuators are required to initiate these yaw and braking maneuvers.

During changes in attitude of a rotor-driven aircraft, gyroscopic forces can occur, which couple the movements around the aircraft's axes, and their influence on the flight motion must be taken into account. Here is an example: After takeoff and before landing, it is necessary to tilt the rotor's axis of rotation by 90° to transit from horizontal flight to vertical flight (or vice versa). This requires a rotation around the pitch axis, which is oriented perpendicular to the direction of propulsion and the vertical axis of rotation. In this transition phase, gyroscopic forces occur because the law of conservation of angular momentum opposes the change in direction. This also applies to rolling. Only in yawing (as described above) does the angular momentum remain directionally stable, and disruptive gyroscopic forces cannot occur.

There are generally two methods for maneuvering under the influence of gyroscopic forces:

1. Utilization of gyroscopic forces;
2. Compensation of gyroscopic forces.

The utilization of gyroscopic forces refers to the exploitation of the UAV's inertia moments to perform maneuvers. By deliberately changing the rotational speeds of the rotors, the UAV can be rotated around its longitudinal, lateral, and vertical axes. This allows for rolling, pitching, and yawing of the UAV. The compensation of gyroscopic forces refers to the mitigation of the undesirable effects of gyroscopic forces to ensure a stable flight attitude. This can be achieved through the use of sensors and control systems that adjust the rotational speeds of the rotors accordingly to compensate for unwanted rotations or vibrations. In our pending patent /19/, it is shown in detail how the maneuverability around all three axes of the UAV can be optimized. The patent specification demonstrates how these two methods can be combined to optimize the maneuverability of the UAV. By strategically utilizing gyroscopic forces and compensating for the undesirable effects, precise and stable maneuvers can be performed.

To find the rotational speed at which the centrifugal force compensates for the weight, we set the following:

$$m_u R(2\pi f)^2 = M g_E$$

This leads to the hovering rotational speed:

$$f^* = \sqrt{\frac{M g_E}{4\pi^2 m_u R}}. \tag{36}$$

To calculate the specific frequency f^*, let us substitute the given values for the medium rotor into the formula:

$$M = 10\text{ kg},\ M = 10^4 * m_u\ (\text{thus } m_u = 1\text{ g}),\ g_E = 9.81\ \frac{m}{s^2},\ \ R = 0.5\text{ m}$$

Substituting these values, we obtain the following:

$$f^* = \sqrt{\frac{10^4 *\ m_u * 9.81 \frac{m}{s^2}}{m_u * 0.5\ m * 4\pi^2}}$$

Calculating this, we obtain:

$$f^* \approx 70.5\text{ Hz}$$

Therefore, the desired frequency f^* is approximately 70.5 Hz (or 4243 rpm).

We need to consider that even during the hovering of the rotor, its rotational energy is consumed because at least the center of mass M is displaced from the axis of rotation by the amount:

$$r = R\frac{m_u}{M} = 0.5\text{ m} * 10^{-4} = 0.05\text{ mm}. \tag{37}$$

This displacement occurs exactly f^* times per second during rotor operation.

To calculate the power consumed during the hovering of the rotor, we use the following formula:

$$P = f^* dE_{rot}. \tag{38}$$

With the energy loss $dE_{rot} = Mg_E r$, we have the following:

$$P = f^* M g_E r. \tag{39}$$

We substitute the given parameter values for the hovering medium rotor. With $1\ W = 1\frac{\text{kgm}^2}{s^3}$, the formula gives the power consumption in watts:

$$P = 70.5\text{ Hz} * 10\text{ kg} * 9.81\frac{m}{s^2} *\ f^* * 0.05 * 10^{-3}\ m\Big) = 0.346\ W$$

To calculate the time that the rotor can hover, we need to calculate the rotational energy reserve. The rotational energy E of a rigid body is given by the following formula:

$$E = \frac{1}{2}\theta\omega^2, \tag{40}$$

where θ is the moment of inertia and ω is the angular velocity. The moment of inertia of a cylinder, which is typically what a rotor is, is calculated using the following formula:

$$\theta = \frac{1}{2}MR^2 \tag{41}$$

where M is the mass, and R is the radius.

The angular velocity ω_0 is equal to $2\pi f_0$, where $f_0 = 400$ Hz is the assumed starting frequency. Substituting the given values into the formulas,

$$\theta = \frac{1}{2} * 10\text{ kg} * 0.5\text{ m}^2 = 1.25\text{ kgm}^2$$

$$\omega_0 = \frac{2\pi * 400}{s} = 800\frac{\pi}{s} = 2512\frac{1}{s}$$

Now, we calculate the rotational energy as follows:

$$E_{rot} = \frac{1}{2} *\ 1.25\text{ kgm}^2 *\ \left(2512\frac{1}{s}\right)^2 = 3{,}943{,}840\ J.$$

The time that the rotor can hover is then the stored rotational energy divided by the power:

$$t = \frac{E_{rot}}{P} = \frac{3{,}943{,}840J}{0.346W} = 11{,}398{,}381 \text{ s. That is approximately 132 days.} \quad (42)$$

This calculation is a strong simplification. In real rotor systems, additional factors such as friction, air resistance, and other losses can dominate and need to be taken into account, too.

6. Precise Control in Activating and Deactivating Rotor Unbalances

The timing and magnitude of the unbalance mass must be adjusted to optimize the propulsion generation. To achieve precise control of the unbalance mass, advanced control systems can be used. These systems monitor the rotational position of the rotor and activate electromechanical actuators to release or adjust the unbalance mass at the desired time and magnitude [19]. Electrically controllable actuators [20] are fixed on the rotor, which applies the piezoceramic length expansion effect (PCT) or the magnetostrictive length expansion effect. The local direction of the length expansion effect must be aligned with the local radial direction of the rotor, causing controlled mass displacement effects towards the rotor periphery and thus causing controlled unbalance (Figure 5).

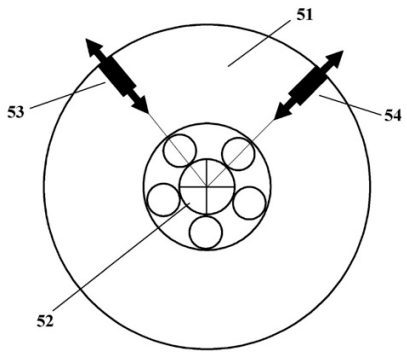

Figure 5. Generation of rotor unbalance (application example): 51 rotor disc, 52 rotor bearing, 53 and 54 unbalance actuators, fixed at the rotor.

The characteristic feature of applying PCT is that the energy requirement for the permanent modulation of the piezoelectric unbalance generator is low because the generator can work highly powerless due to the high PCT internal resistance. Furthermore, the piezoelectric effect allows for rapid changes in unbalance. Possible PCT length changes are in the order of a few 100 µm, with mechanical response times of only 10^{-4} s or less. Furthermore, the characteristic feature of the piezoelectric unbalance generator is that rotations with frequencies of 10 kHz and higher become technically possible. Therefore, we conclude that by applying rotors equipped with current bearing technology, the unbalance control could be realized up to rotor speeds of about 1000 rps, and even higher speeds are possible for magnetically levitated rotors. Note that during accelerated flight, only unbalance-induced inertial forces act on the rotor bearing, as the elastic support forces are eliminated when the rotor fixation is released. As a result, the load on the bearings due to unbalance is significantly smaller during flight compared to the operation of a tethered rotor. This is expected to have a favorable effect on the service life, especially for roller bearings.

7. High-Strength Rotor Materials

For high-speed rotors high tensile strength and low material density of the rotor material applied are essential. In designing a propulsion system, the following criterion of

strength theory must be considered: In a high-speed rotating rotor (balanced), the tangential component of the surface stress s_t must not exceed the tensile strength of the rotor material:

$$s_t = \rho\, v^2 R < maximum\ tensile\ strength\ s_{max} \tag{43}$$

The component of the surface stress s_t itself is proportional to the material density ρ and the square of the circumferential velocity v_R of the rotor. This is determined by:

$$v_R = 2\pi R f \tag{44}$$

Therefore, we have the following:

$$4\pi^2 f^2 R^2 < s_{max}$$

$$fR < \frac{1}{2\pi} * \sqrt{\frac{s_{max}}{\rho}} \tag{45}$$

This formula says the optimized rotor material should have tensile strength s_{max} as large as possible, and its density ρ should be as low as possible. Rotors built by using this optimized material allow large magnitudes of the critical product fR, i.e., high rotation frequencies f in combination with the large radius R of big-sized rotors. Permissible tensile strength should include additional stresses by the centrifugal force of the unbalanced mass.

Our calculation results for some metallic materials and for carbon nanomaterials are shown in Figure 6:

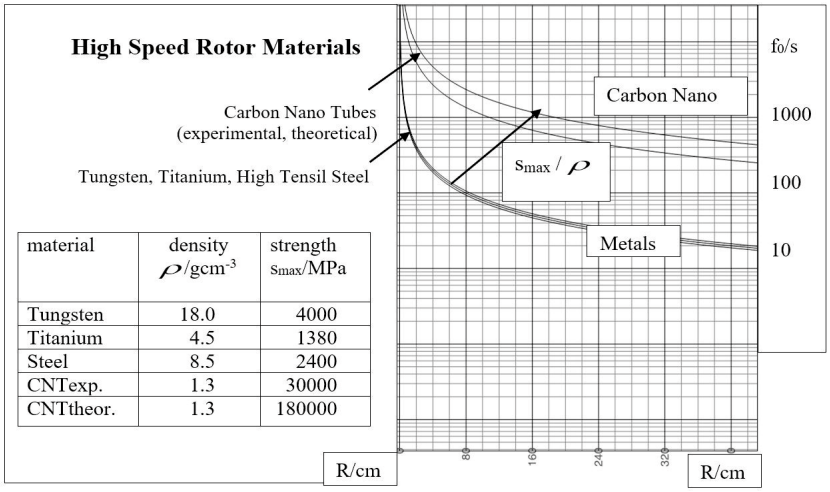

Figure 6. Highest rotation frequencies $\frac{f_0}{s}$ in dependence of radius R and parameter $\frac{s_{max}}{\rho}$ for selected materials according to Equation (45), material data according to [21–24].

We draw the following conclusion: Using present metallic rotor materials, radii in the sub-meter range can be achieved for speeds of 100–1000 rps, especially with carbon-fiber-reinforced polymer (CFRP) wrapped steel rotors, as described in [21]. Furthermore, based on some success in younger experiments with nanomaterials [21–23], single-walled carbon nanotubes theoretically possess ultimate intrinsic tensile strengths in the 100–200 GPa range, among the highest in existing materials. We are so free to state here: The highest rotor speeds (1000 rps) could be achieved when using ultra-stabile carbon nanomaterial structures because this technology could be combined with allowable rotor radii in the order of several meters. Let us compare these demands to the state-of-the-art rotor equipment: CNC tool machine spindles (80 mm) make 250 rps, standard commercial high-speed ball bearings perform 350 rps, and magnetic bearings work up to 500,000 rpm, and more; see [14,25].

Of course, there is always an alternative way of creating high thrust by means of pulse-modulated force propulsion: Instead of a single super rotor with a large radius, a battery of several smaller rotors (mounted on a common vehicle platform) can be applied, operated with synchronous unbalance control so that the individual propulsion forces add up.

8. Final Conclusions

Pulsed centrifugal propulsion is based on well-established laws of physics, i.e., the energy theorem, the principle of linear and rotational momentum, and Newton's axioms. We provide traceable evidence that the propulsion of small vehicles (UAV) can be generated by the conversion of the rotational energy of airborne rotors. By precise seting/resetting unbalances during each rotor rotation, short centrifugal force pulses can be induced and exactly directed. Thus, by controlled unbalance propulsion (CUP), the rotational energy of a rotor can be transformed into translational energy of the rotor-carrying vehicle.

Furthermore, we conclude that controlled unbalance propulsion could provide excellent flight performance data for small UAVs. Our calculations indicate that high thrusts and vehicle velocities up to orbital levels could be achieved. Thus, the working range of high-performance CUP drones could be extended to near-Earth space and seems not limited to Earth's atmosphere. Additionally, exceptional maneuverability and levitation can be attained, making these UAVs superior to conventional drones. Targeted action in the design and performance dimensioning of centrifugal force drives is possible based on this information. This paper allows for specific actions to be taken when designing and determining the performance of centrifugal force drives. The practicability of inertial drives can be tested with state-of-the-art components.

Last but not least, a second CUP generation applying combined inertial/electric propulsion of vehicles appears to be feasible. Here, the unbalance-controlled rotor is part of an electric motor drive/generator circuit. Initially, additional electrical power is stored in (low-weight) onboard batteries during the prestart phase. This process occurs in parallel with the electrical loading of the rotor to its maximum rotation frequency, ω_0. Later, during flight, the stored electrical energy can be used to compensate for the decrease in rotational energy during the vehicle's thrust phases. This allows the rotor to maintain a constant frequency, ω_0, during vehicle operation, which should simplify the guidance software and energy management. Furthermore, due to the increase in total onboard energy, the operational range of the vehicle should be expanded.

Funding: This research received no external funding.

Institutional Review Board Statement: Not applicable.

Informed Consent Statement: Not applicable.

Data Availability Statement: The raw data supporting the conclusions of this article will be made available by the authors on request.

Conflicts of Interest: The author declares no conflicts of interest.

References

1. Slowronscy, M.J. Impulse Momentum Propulsion Apparatus and Method. U.S. Patent 000551A1, 11 January 2018.
2. Woodward, J.; Mahood, T. Method and Apparatus for Generating Propulsive Forces without the Ejection of Propellant. U.S. Patent 6347766B1, 13 February 2002.
3. Cook, R.L. Device for Conversion of Centrifugal Force to Linear Force and Motion. U.S. Patent 4238968A, 16 December 1980.
4. Dean, N.L. System for Converting Rotary Motion into Unidirectional Motion. U.S. Patent 2,886,976, 19 May 1959.
5. Zhang, B.; Song, Z.; Zhao, F.; Liu, C. Overview of Propulsion Systems for Unmanned Aerial Vehicles. *Energies* **2022**, *15*, 455. [CrossRef]
6. Joshi, D.; Deb, D.; Muyeen, S.M. Comprehensive Review on Electric Propulsion System of Unmanned Aerial Vehicles. *Front. Energy Res.* **2022**, *10*, 752012. [CrossRef]
7. Gur, O.; Rosen, A. Optimizing Electric Propulsion Systems for Unmanned Aerial Vehicles. *J. Aircr.* **2009**, *46*, 1340–1353. [CrossRef]

8. Mousavi G, S.M.; Faraji, F.; Majazi, A.; Al-Haddad, K. A comprehensive review of Flywheel Energy Storage System technology. *Renew. Sustain. Energy Rev.* **2017**, *67*, 477–490. [CrossRef]
9. Li, X.; Palazzolo, A. A review of flywheel energy storage systems: State of the art and opportunities. *J. Energy Storage* **2022**, *46*, 103576. [CrossRef]
10. Yu, S.; Guo, W.; Teng, Y.; Sang, W.; Cai, Y.; Tian, C. A review of the structures and control strategies for flywheel bearings. *Energy Storage Sci. Technol.* **2021**, *10*, 1631–1642. [CrossRef]
11. Karrari, S.; De Carne, G.; Noe, M. Model validation of a high-speed flywheel energy storage system using power hardware-in-the-loop testing. *J. Energy Storage* **2021**, *43*, 103177. [CrossRef]
12. Karrari, S.; Noe, M.; Geisbuesch, J. Real-time simulation of high-speed flywheel energy storage system (FESS) for distribution networks. In Proceedings of the 9th ACM International Conference on Future Energy Systems, e-Energy 2018, Karlsruhe, Germany, 12–15 June 2018; ISBN 978-1-4503-5767-8; KITopen-ID 1000085091.
13. Flywheel-Generators. Max Planck Institute for Plasma Physics. 2021. Available online: https://www.ipp.mpg.de/4244138/generatoren (accessed on 14 May 2024).
14. Buchroithner, A. *Flywheel Energy Storage in Automotive Engineering*; Springer: Berlin/Heidelberg, Germany, 2023; p. 327, ISBN 3658353414/978-3658353414.
15. Halliday, D.; Resnick, R.; Walker, J. *Fundamentals of Physics*, 10th ed.; John Wiley & Sons: Hoboken, NJ, USA, 2013; p. 1456, ISBN 111823071X/978-1118230718.
16. Taylor, J.R. *Classical Mechanics*, 1st ed.; University Science Books: Sausalito, CA, USA, 2005; p. 802, ISBN 189138922X/978-1891389221.
17. Demtröder, W. *Physik für Ingenieure*, 4th ed.; Springer: Berlin/Heidelberg, Germany, 2010; p. 630.
18. Schneider, H. *Auswuchttechnik*, 9th ed.; Springer: Berlin/Heidelberg, Germany, 2021.
19. Holzapfel, W. Verfahren zur Vortriebserzeugung. DE Patent 10 2021 004 170 A1, 16 February 2023.
20. Wang, Z.L.; Zhang, Y.; Hu, W. *Applications to Third Generation Semiconductor Microtechnology (Microtechnology and MEMS)*; ASIN:B0C3WZNKY8; Springer: Berlin/Heidelberg, Germany, 2023.
21. Bai, Y.; Zhang, R.; Ye, X.; Zhu, Z.; Xie, H.; Shen, B.; Cai, D.; Liu, B.; Zhang, C.; Jia, Z.; et al. Carbon nanotube bundles with tensile strength over 80 GPa. *Nat. Nanotechnol.* **2018**, *13*, 589–595. [CrossRef] [PubMed]
22. Takakura, A.; Beppu, K.; Nishihara, T.; Fukui, A.; Kozeki, T.; Namazu, T.; Miyauchi, Y. Strength of carbon nanotubes depends on their chemical structures. *Nat. Commun.* **2019**, *10*, 3040. [CrossRef] [PubMed]
23. Ruoff, R.S. Strong bundles based on carbon nanotubes. *Nat. Nanotechnol.* **2018**, *13*, 533–534. [CrossRef] [PubMed]
24. Granta Design Limited. *Cambridge Engineering Selector Software*, CES 4.1; Granta Design Limited: Cambridge, UK, 2003.
25. Schuck, M.; Steinert, D.; Nussbaumer, T.; Kolar, J. Ultrafast rotation of magnetically levitated macroscopic steel spheres. *Sci. Adv.* **2018**, *4*, e1701519. [CrossRef] [PubMed]